Scanning Microscopy, Vol. 1, No. 3, 1987 (Pages 901-909)
Scanning Microscopy International, Chicago (AMF O'Hare), IL 60666 USA

0891-7035/87$3.00+.00

DEVELOPMENT OF AN ULTRA HIGH RESOLUTION SCANNING ELECTRON MICROSCOPE BY MEANS OF A FIELD EMISSION SOURCE AND IN-LENS SYSTEM

Takashi Nagatani*, Shoubu Saito
Mitsugu Sato, and Mitsuhiko Yamada

Naka Works, Hitachi Ltd.
882 Ichige, Katsuta, Ibaraki 312 Japan

(Received for publication January 28, 1987, and in revised form April 28, 1987)

Abstract

An ultra high resolution scanning electron microscope, which is composed of a cold cathode field emission gun and an in-lens system for specimens, has been developed. Probe size is estimated 0.8nm at 30kV by calculation and confirmed experimentally using high atomic number samples such as fine Pt particles sputter-coated on carbon. Three stage ion pumps for the column and a turbo molecular pump for the specimen chamber have been used for a totally dry vacuum system. Applications for fine metal oxide particles and biological samples observed directly without any metal coating, and applications chosen especially to show lower voltage performance, are shown.

Key Words: High resolution scanning electron microscope, field emission scanning electron microscope, in-lens field emission electron microscope, side-entry stage, Pt particles, Au-Pd particles, MgO, ZnO, intestinal microvilli (mouse).

*Address for correspondence:
Takashi Nagatani
Hitachi Ltd. - Naka Works
882 Ichige, Katsuta, Ibarakai 312
Japan

Phone number: 81-292-73 2111

Introduction

It has been generally accepted for years that the resolution limit of scanning electron microscopes (SEM) might not be better than 1nm because of the escape depth of the secondary electrons from a solid surface. After an experiment conducted by authors [6] with the "zero working distance" method on a conventional field emission SEM (FESEM), which had a resolution of about 1.5nm at 30kV and was verified by Tanaka [11], the recent experiment by means of the "in-lens FESEM" (samples are set inside the pole pieces of a highly excited objective lens of a field emission SEM) shows that it seems possible to achieve a resolution of better than 1nm [9]. Kuroda and Komoda [5] have also experimented with similar construction of an FESEM (a modified STEM) and observed an atomic layer, 4.5 Å step of a surface of tungsten monocrystal tip.

Tanaka et al [12] have developed an in-lens FESEM (model UHS-T1 installed at Tottori University), which has a beam diameter of 0.5nm at 30kV. Some high magnification micrographs of biological samples have already been reported [13]. Following this, we have developed a commercialized type of "In-lens FESEM", model S-900 [7], as shown in Fig. 1. The details of the instrumentation and applications are described here.

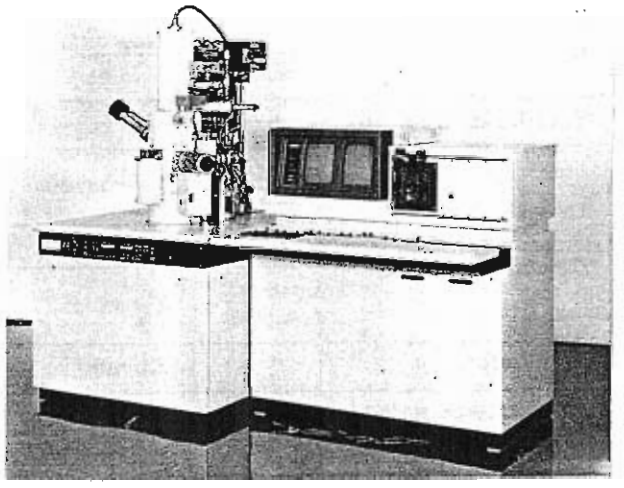

Fig. 1. Outer view of an in-lens FESEM, model S-900.

Electron optics system

Fig. 2 shows a cross-sectional view of the column. The electron source is a cold field emission type utilizing a single crystal tungsten tip of (310) orientation. The electron gun is composed of a cold emitter cathode, and first and second anodes.

The accelerating voltage is applied on the second anode and is variable from 1kV to 30kV, in a small incremental step of 100V/step for 1 through 5kV and 1kV/step for 6 through 30kV. The first and the second anodes work as an electrostatic lens so we have employed the Butler type design which assures the smallest aberrations. In order to operate the field emitter properly, it is necessary to flash the tip of the cathode, apply and regulate the first anode voltage to secure emission current of about 10 μA, and apply the required accelerating voltage (V_0) on the second anode. All of these operations are automatically performed by a built-in microprocessor.

The lens system is composed of condenser, intermediate and objective lenses. The condenser lens is used to focus the electrons emitted from the gun and to regulate the probe current. The probe current is variable in 14 discrete steps. Since the first and second anodes work as a static lens, the virtual source position of the electron beam with respect to the condenser lens changes with a change of the first and second anode voltages (Fig. 3). We have used a built-in computer to locate the virtual source and regulate the condenser lens excitation accordingly.

The objective lens is the most critical factor for the image resolution. We have decided to use our objective lens at a focal length of 3.6mm for the smallest aberrations. For this reason, it is necessary to position the specimen in the pole piece gap. The shape of the pole piece is directly associated with aberrations. We have used computer simulation to determine the optimum shape and dimensions and have achieved spherical aberration (C_S) of 1.9mm, and chromatic aberration (C_C) of 2.6mm at a focal length of 3.6mm (Table 1). For stereoscopic image recording, an eucentric goniometer specimen stage was devised to permit specimen tilting on a focal plane of the objective lens.

Table 1. Specifications for the objective lens of S-900

Specifications for Objective lens		
Designed shape of Objective Pole piece	Upper Polepiece	10 mmϕ dia.
	Gap	11 mm
	Lower Polepiece	2 mmϕ dia.
Focal length	f	3.6 mm
Spherical Aberration Coefficient :	C_s	1.9 mm
Chromatic Aberration Coefficient :	C_c	2.5 mm

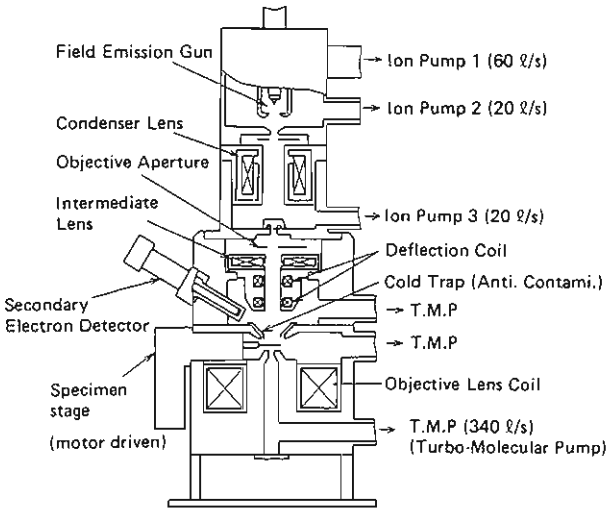

Fig. 2. Cross-sectional view of the column.

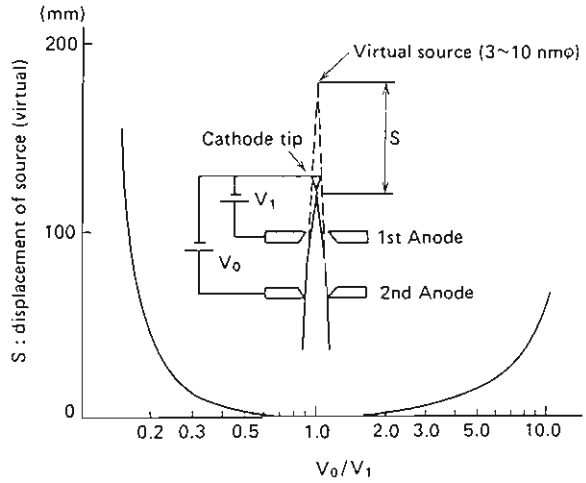

Fig. 3. Displacement of virtual source position with respect to the voltage ratio V_0/V_1.

The scanning of the electron beam is done by a 2-stage deflector coil. We have used computer simulation to find a stationary point for beam scan with the smallest aberration. While the optimum deflection fulcrum is generally in the vicinity of the principal plane of the objective lens, the optimum is not always the principal plane. In the S-900 objective lens, the optimum fulcrum is about 4mm above the specimen. There is no pin-cushion nor barrel distortion caused at this point. However, a large deflection angle is difficult due to the short distance between the fulcrum and the specimen. We have decided to use a 2-stage deflection for 250X or higher magnifications and a 1-stage deflection for magnifications below 250X. For low magnification work, the objective lens is weakly excited and focusing is done by the intermediate lens (Fig. 4).

There are two good reasons for using the objective lens at a weakly excited condition for a 1-stage beam deflection. The first reason is to utilize the magnetic field of the objective lens for efficient secondary electron collection. The second reason is

to compensate for the image rotation while going from the 1-stage to the 2-stage deflection operation or vice versa. The image rotation angle is proportional to the lens excitation. Therefore, it is possible to set an excitation condition at the 1-stage deflection such that there is no image rotation in the 2-stage deflection mode. There is a way to compensate for the image rotation by energizing the beam deflector coil with a rotation signal, but it is much simpler to use the objective lens excitation condition.

Signal detection and specimen stage

The secondary electrons emitted from the specimen are collected with a detector positioned above the objective lens. This is a necessary requirement for a system in which the specimen is positioned in the pole piece gap. The secondary electrons are pulled up by the magnetic field of the objective lens. The higher the magnetic field, the better the secondary electron collection efficiency. At high accelerating voltage operation, the secondary electron detector needs to be positioned close to the electron optical axis. However, the high voltage (10kV) applied on the secondary electron detector can cause alignment problems at a low accelerating voltage operation. The S-900 has a secondary electron detector which can be repositioned for low voltage (1kV through 5kV) and medium/high voltage (6kV through 30kV) operation and it ensures high performance at all working voltages.

Specimen stage design is similar to a side-entry stage for TEMs, because the specimen must be set inside the objective lens (Fig. 5).

Spot size of the beam

In general, the resolution of a SEM depends upon the nature of the sample. That is, the contrast of topographic details of the sample surface determine the actual visibility. The resolution can never be better than the spot size of the beam. However, it would seem logical to specify the spot size first when designing a high resolution SEM.

The spot size of the beam is mainly limited by spherical aberration and diffraction at accelerating voltages higher than 10kV. Chromatic aberration and diffraction, on the other hand, are the dominant factors at accelerating voltages lower than 5kV. Source size of a cold field emission is so small that we could neglect it for simplicity. Then, the root mean square (R.M.S.) method will give us a rough spot size. However, R.M.S. should not be used to combine these various aberration effects to estimate the spot size correctly, since the effects are not statistically independent and are based upon different concepts, ranging from geometrical optics to wave optics.

Crewe [2] proposed that the O.T.F. (optical transfer function) of a wave optics method must be used to evaluate the spot size. Fig. 6 shows these calculated spot sizes for various accelerating voltages.

Fig. 6. Calculated probe size radius R at different accelerating voltages V_0; classical R.M.S. method, 0.43 $Cs^{1/4}\lambda^{3/4}$ as STEM, and the value estimated by considering wave optics.

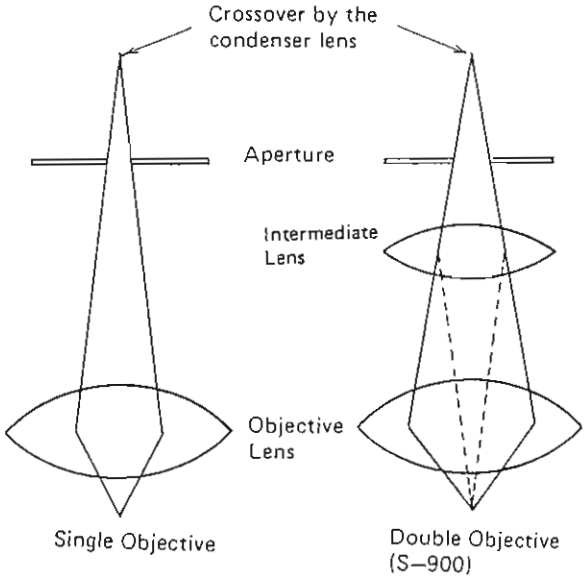

Fig. 4. Use of intermediate lens for lower magnification range and also for the compensation of image rotation.

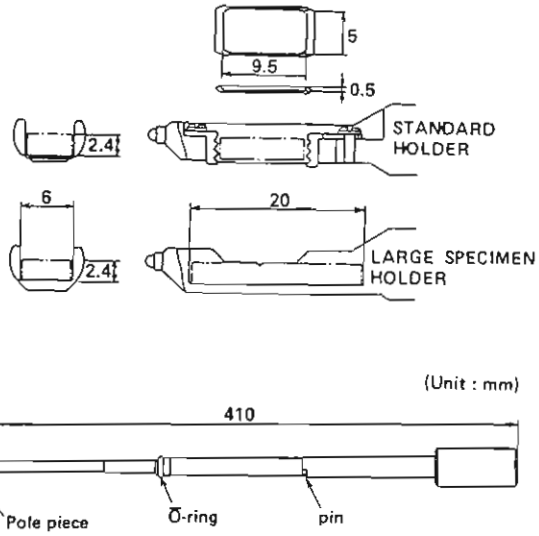

Fig. 5. Specimen holder for side-entry system.

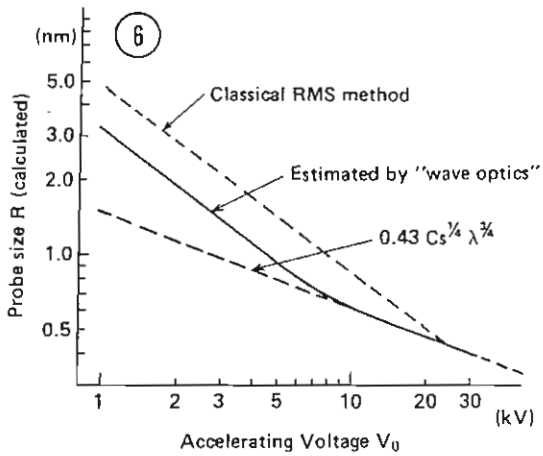

Evacuation System

An oil-free evacuation system is used as shown in Fig. 7 to minimize contamination. The gun chamber and the column are evacuated with three ion pumps and the specimen chamber is pumped by a turbo molecular pump. The pressure ultimately becomes 1 X 10^{-7} Pa in the gun chamber and is in the low 10^{-5} Pa range in the specimen chamber.

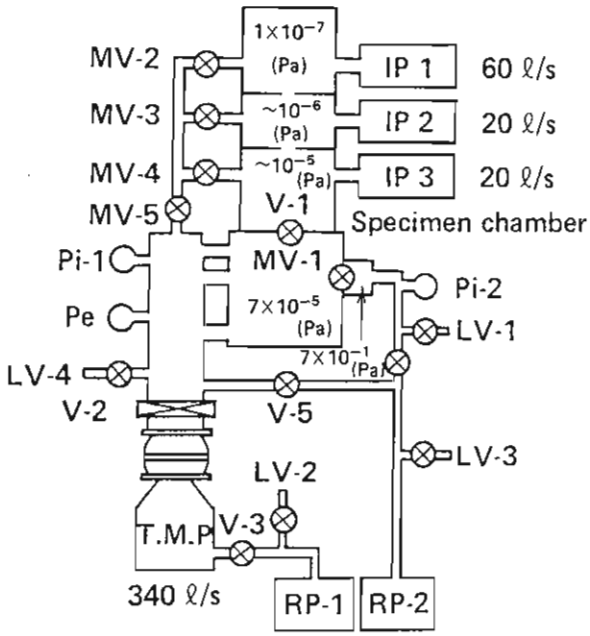

Fig. 7. Vacuum system for the column.

Applications

Platinum and Gold-Palladium particles on carbon flakes

Fine particles of Pt and Au-Pd sputter-evaporated on carbon flakes were observed for evaluating the resolving power of the SEM. This kind of sample is suitable for estimating the probe size. The smallest particles we could see were less than 1nm at 30kV (Fig. 8a) and about 4nm at 1kV (Fig. 8b).

Oxide iron particles

Fine details of iron oxide powder were directly observed at lower voltage (2kV) to avoid the so-called "Accelerating Voltage Effect" (Fig. 9).

MgO crystals

Fine particles of magnesium oxide crystal have been well known as a typical test sample in transmission electron microscopy (TEM). For example, Fukami [3] and Adachi et al. [1] used them for evaluating the resolution limit of replica technique. We observed them for evaluating the SEM resolution and for making comparisons with replicas.

MgO particles were directly deposited on a copper mesh, commonly used for the TEM, by simply burning magnesium ribbon in atmosphere. The mesh was mounted on a side-entry stage and directly observed at magnifications up to X800,000 without performing any pre-treatment such as metal coating [8].

Fig. 10a is a typical SEM micrograph for a fairly large MgO cubic crystal, in which multiple steps, parallel to the (001) plane, are clearly observed. Part of these steps are magnified in Fig. 10b. Then, we tried to observe a smaller cube crystal shown in Fig. 10c, which was attached to the tilted surface of a large crystal shown in Fig. 10d.

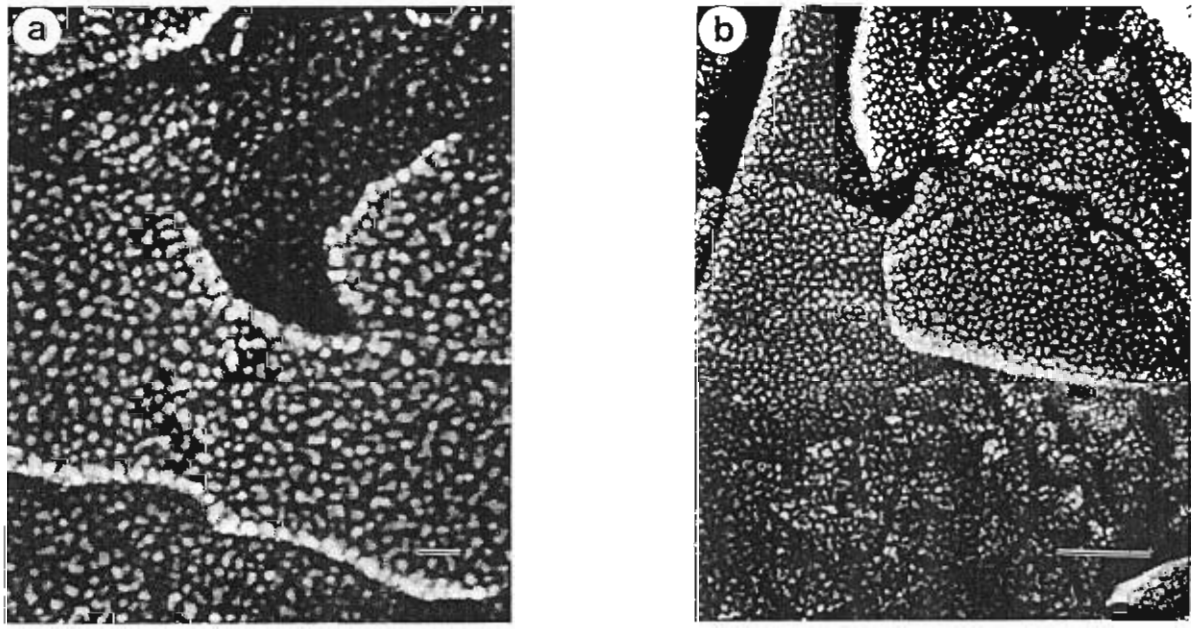

Fig.8. Resolution test sample; (a) Pt sputter coated on carbon, taken at 30kV. Bar = 10nm. (b) Au-Pd sputter coated on carbon, taken at 1kV. Bar = 100nm. Specimens were heated at 150°C during photographing (50 sec/frame) to avoid contamination.

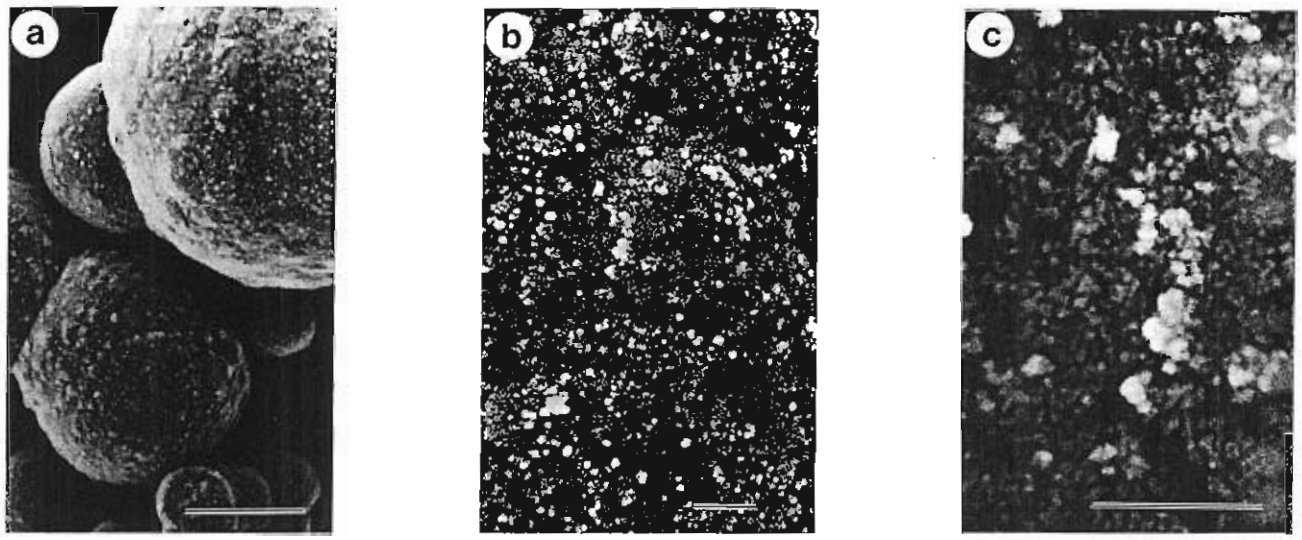

Fig. 9. Direct observation of iron oxide; (a) taken at 2kV, bar = 1 μm; (b) taken at 2kV, bar = 100nm; (c) taken at 2kV, bar = 100nm.

MgO crystals are quite useful in evaluating the SEM performance. For example, an effective probe size could be estimated from the SEM micrograph by considering the degraded sharpness of the vertex of the crystal at high magnification. This sharpness appears superior to the resolution of the replica-TEM method by which Fukami [3] and Adachi et al. [1] estimated the resolution to be about 2.5nm. For comparison, a direct carbon replica taken by TEM is shown in Fig. 10e.

A strict comparison for microtopographical studies between direct observation by high resolution SEM and replica-TEM methods will be required for various materials.

ZnO crystals

Fig. 11a, c and d show ZnO crystals which were prepared as the MgO mentioned above and directly observed by the S-900. Micrographs were also taken by 200kV TEM for comparison and are shown in Fig. 11b. It should be noted that some of the crystal steps observed in the SEM micrograph on the stem of the whiskers could hardly be observed by TEM.

Low voltage applications for biological samples

Enteric surface coat (glycocalyx) of small intestinal microvilli (mouse) prepared by a conductive staining, by Takahashi [10], which is composed mainly of the tannin-ferrocyanide-OsO_4 method, was directly observed at 2kV and is shown in Fig. 12.

Conclusion

Ultra high resolution SEM experiments were performed with a so-called "in-lens FESEM". It has the ability to observe fine particles less than 1nm in diameter and fine crystallographic steps which could hardly be seen by ordinary TEM. The ultra high resolution FESEM is now a competitor with other high resolution techniques such as low loss electron (LLE) imaging [14] and reflection electron microscopy (REM) [4]. One of its important applications is to respond to an increasing demand for a high resolution, low voltage SEM in order to observe a sample surface without coating for new materials. This will be described in a separate paper, especially, for recent semiconductor materials and submicron devices.

Acknowledgements

The authors sincerely thank Prof. K. Tanaka and his group at Tottori University for their cooperative work in developing the high resolution SEM and Prof. A.V. Crewe of the University of Chicago for his advice and discussions on theoretical ultimate resolution of the SEM. Thanks are also due to Dr. G. Takahashi of Hirosaki University School of Medicine for preparing a sample, and to Drs. T. Komoda and K. Kuroda of the Central Research Laboratory for their assistance in developing UHR-FESEM, and to our instrument designer group, M. Kanda, M. Matsui, M. Nakaizumi, and the application engineers T. Watanabe and T. Suzuki for their support.

References

1. Adachi K, Honjou K, Katoh M, Kanaya K (1976). High resolution shadowing for electron microscopy by sputter deposition. Ultramicroscopy 2, 17-29.

2. Crewe AV (1985). Towards the ultimate scanning electron microscope. Scanning Electron Microsc. 1985; II: 467-476.

3. Fukami A (1958). A high resolution pre-shadowed carbon replica method and its direct stripping technique. J. Electron Microscopy 6, 18-24.

4. Hsu T, Cowley JM (1983). Reflection electron microscopy (REM) of fcc metals. Ultramicroscopy 11, 239-250.

5. Kuroda K, Komoda T (1985). Observation for crystal surface of W <110> field emitter tip by SEM. J. Electron Microscopy 34, 179-180.

6. Nagatani T, Okura A (1977). Enhanced secondary electron detection at small working distance in the field emission SEM. Scanning Electron Microsc. 1977; I: 695-702.

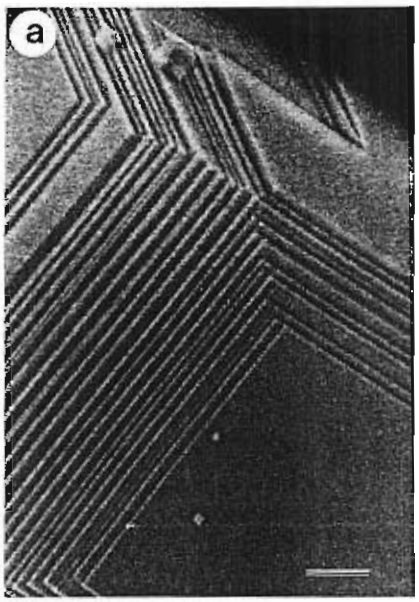

Fig. 10. Direct observation of MgO; (a) and (b) crystal step taken at 10kV, bar = 100nm; (c) a small cubic crystal (bar = 20nm) attached to a large crystal shown in (d); (d) bar = 200nm; (e) direct carbon replica taken by TEM, bar = 20nm.

Fig. 11. Direct observations of ZnO; (a) by SEM taken at 5kV, bar = 200nm; (b) by TEM taken at 200kV, bar = 200nm; (c) and (d) magnified images showing crystal steps, bar = 100nm.

Fig. 12. Enteric surface coat (glycocalyx) of small intestinal microvilli (mouse) prepared by tannin-ferrocyanide-OsO_4 method (Takahashi [10]) directly observed at 2kV, uncoated. Bar = 100nm.

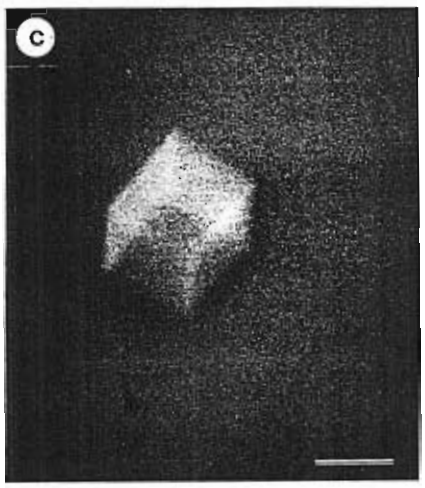

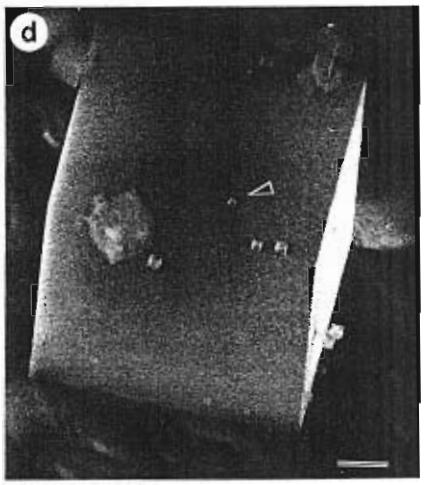

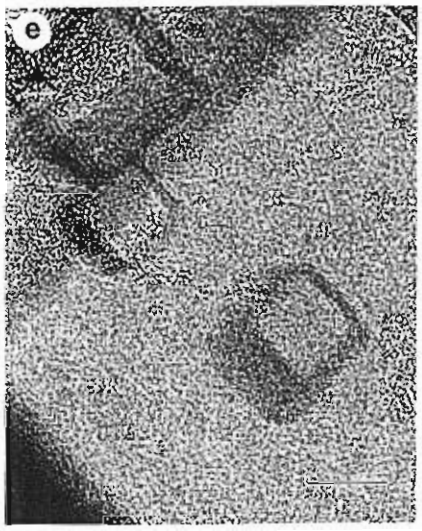

7. Nagatani T, Saito S (1986). Instrumentation for ultra high resolution scanning electron microscopy. Proc. 11th Internatl. Cong. on Electron Microscopy, Kyoto. J. Electron Microscopy supplement 35, 2101-2104.

8. Nagatani T, Suzuki T, Yamada M (1986). Direct Observation of magnesium oxide crystal by means of a high resolution SEM. J. Electron Microscopy 35, 208-209.

9. Nagatani T, Yamada M, Saito S, Nakaizumi Y (1983). An experiment on ultra high resolution SEM. Seiran-Kai, Tottori University, School of Medicine. Japan, 8-9.

10. Takahashi G (1986). Tannin-ferrocyanide-OsO_4 method for transmission and scanning electron microscopy. Proc. 11th Internatl. Cong. on Electron Microscopy, Kyoto. J. Electron Microscopy supplement 35, 2175-2176.

11. Tanaka K (1981). Demonstration of intracellular structures by high resolution scanning electron microscopy. Scanning Electron Microsc. 1981; II: 1-8.

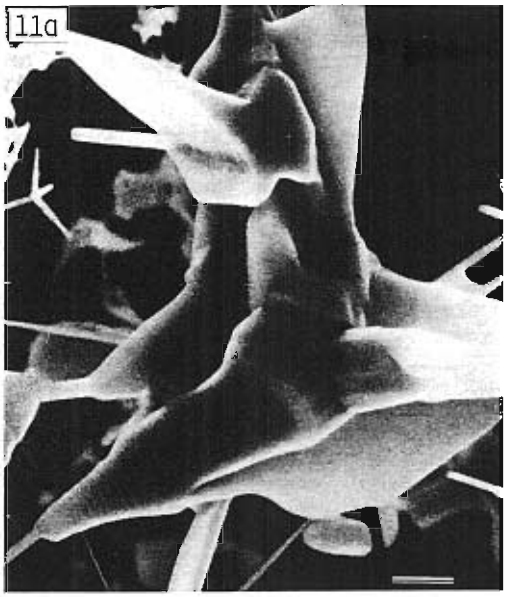
11a


11b

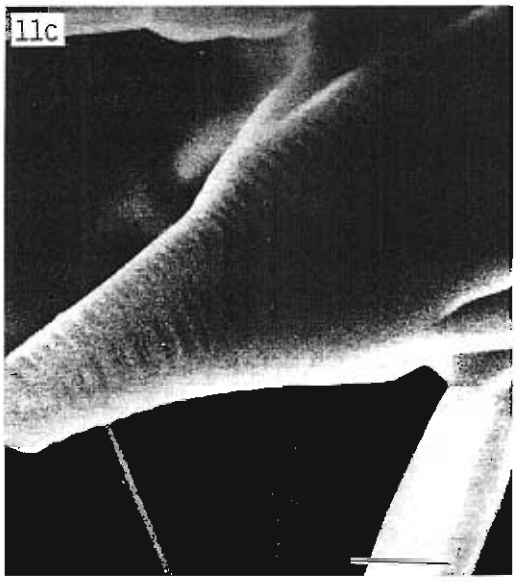
11c

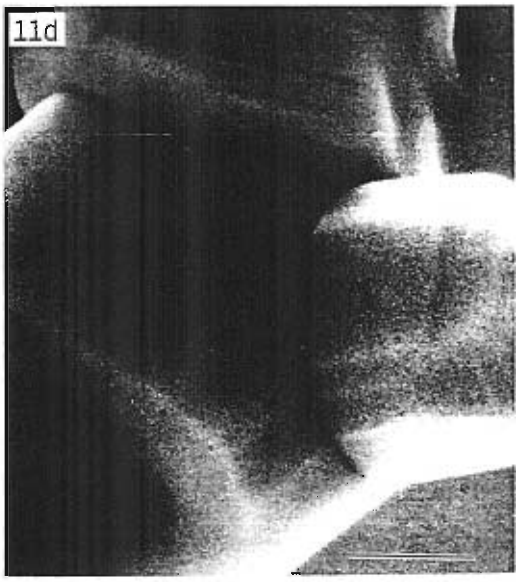
11d

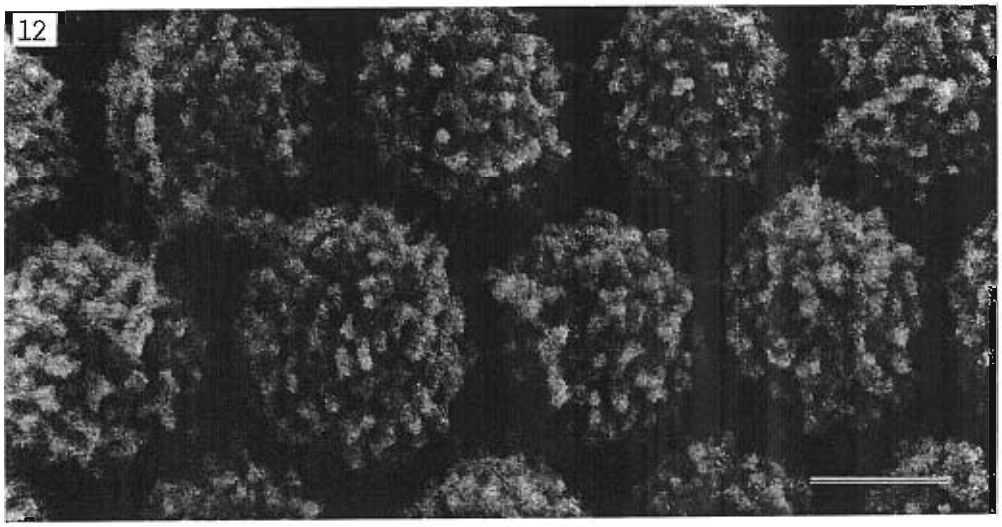
12

12. Tanaka K, Matsui I, Mitsushima A, Nagatani T (1986). Ultra high resolution SEM. Ohyo Butsuri (in Japanese) 35, 31-35.

13. Tanaka K, Mitsushima A, Kashima Y, Osatake H (1986). A new high resolution scanning electron microscope and its application to biological materials. Proc. 11th Internatl. Cong. on Electron Microscopy, Kyoto. J. Electron Microscopy supplement 35, 2097-2100.

14. Wells OC (1986). Low-loss electron images of uncoated photoresist in the scanning electron microscope. Appl. Phys. Lett. 49[13], 764-766.

Discussion with Reviewers

J.M. Cowley: Fig. 6 shows estimated resolution found by wave optics. How were the chromatic aberration effects taken into account theoretically if not by the R.M.S. method?
Authors: The O.T.F. in the spatial frequency which corresponds to the Rayleigh criterion ($0.61\lambda/\alpha$) shows 0.089 at the image point of Gaussian optics. In low accelerating voltage operation, in which the effect of spherical aberration is almost negligible, there exists some plateau area of spatial frequency (see Figure) when we plot the equi- O.T.F. (at 0.089) curve along the optical axis and there is no degradation of resolution on that plateau.

The plateau can be varied by α (aperture angle). If we make it (plateau) wider than Δ fc (defocus due to chromatic aberration), the resolution does not deteriorate because of chromatic aberration. Therefore, if we control α so as to make the plateau coincide with Δ fc, e.g., an optimum aperture α_{opt}, theoretical resolution can be obtained by:

$$0.61\lambda/\alpha_{opt} = 0.55\,(C_c \Delta E/E)^{1/2}$$

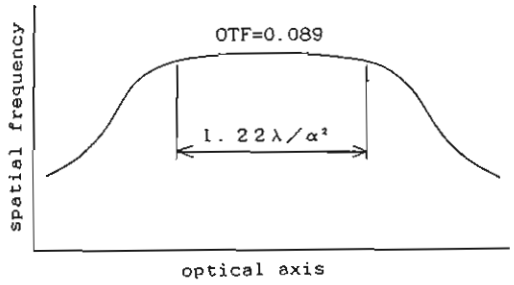

T. Mulvey: In Figure 6 you refer to the middle curve as being "Estimated by wave optics". The lower curve ($0.43\,C_s^{1/4}\lambda^{3/4}$) is also clearly based on wave optics. Why are the curves different?
Authors: It is evident that the evaluation by $0.43C_s^{1/4}\lambda^{3/4}$ is valuable only at higher voltage where the spherical aberration is dominant, and is not applicable at lower voltage, where the chromatic aberration is dominant. So, we should consider some deterioration of the probe size due to the chromatic aberration (see also answer to previous question).

J.M. Cowley: Is it possible in this microscope to insert a secondary electron detector below the specimen so that both sides of a transmission specimen may be seen? Also, is it possible to detect back-scattered and forward scattered fast electrons?
Authors: Both transmitted electron detector and back-scattered electron detector made of YAG scintillator can be provided. However, there is no detector for the forward scattered fast electrons.

T. Mulvey: You state that you used the "Butler type design" of field ion gun that "assures the smallest aberration". Munro showed many years ago that this design, although quite acceptable, is not in fact an optimum design. Secondly, do you think that the aberrations of the field emission gun itself influence, in any way, the performance of the instrument when operating in the "high resolution" mode? It would seem unlikely at first sight.
Authors: Spherical aberration caused by the field emission gun (FEG) has little effect on the final resolution (less than 0.1nm by calculation). On the other hand, even though chromatic aberration of the FEG adds several angstroms to the final probe size at 1kV, there is practically no deterioration of the resolution.

T. Mulvey: In Fig. 8, it is stated that the sample was heated to 150°C to reduce contamination. What is the origin and extent of this contamination? I presume you have a very good vacuum in order to have stable operation of the field emission gun.
Authors: We have a totally dry system using an ion-getter pump and a turbo-molecular pump even for the specimen chamber itself. So, the deposition rate of the contamination very much depends upon the sample. However, there is no practical effect due to the sample on the vacuum quality, especially, in the gun chamber ($\sim 10^{-8}$ Pa) due to the three stages of differential pumping (see Fig. 7).

T. Mulvey: Can you expand the very brief remarks on the arrangement of the secondary electron detector which is crucial for the successful operation of this instrument? In the diagram of figure 2, the detector seems too far away to be effective in collecting the secondary electrons trapped by the strong axial magnetic field.
Authors: As shown in Fig. 2, the post-acceleration voltage applied to the scintillator of the secondary electron detector deflects the scanning beam and may increase off-axis aberrations and thus degrade the resolution. There exists a serious trade-off between detection efficiency and resolution, especially at lower voltages (less than about 5kV). So, we designed a retractable system which allows the distance between the optical axis and the detector to be varied from 40mm (5-30kV) to 60mm (<5kV).

D.C. Joy: Have you any information about the shape of the beam profile, particularly at low beam energies? Is it Gaussian, and if not, do you feel that this is a disadvantage?
Authors: The profile of a perfectly coherent beam can easily be estimated at any point on the optical axis. It is almost Gaussian at the focal plane, but strictly speaking, it is not Gaussian (Max Born and Emil Wolf, Principles of Optics. Pergamon Press, Oxford 1975, Chapter 8, 8.5 Fraunhofer Diffraction). The profile of a beam having chromatic aberration can probably be calculated from a coherent beam profile which is properly modified in its energy distributions. It needs enormous effort, and we did

not do it yet. However, it is evident that if we superimpose profiles which are not Gaussian, the final profile is not Gaussian. We really do not know which is better, Gaussian or non-Gaussian.

D.C. Joy: What control does the operator have over the convergence of the incident beam?
Authors: Although the operator always controls the same knobs for focussing, the objective lens current is adjusted in the case of 2-stage deflection and the intermediate lens current is adjusted for 1-stage deflection. These are switched over automatically by microprocessor.

D.C. Joy: Is spot size, or stage vibration, the factor currently limiting performance of this instrument? What would you predict the resolution to be at, say 50keV, taking both factors into account?
Authors: The resolution is not limited by stage vibration but spot size, since, like the TEM case, the side-entry stage is fairly resistant to outside disturbance. We have not yet experimented with this system at 50kV.

J.C. Wiesner: Relative to the field emission source, please describe briefly:
(a) Useful working time between flashes.
(b) Typical peak-to-peak focussed probe current fluctuations without compensation.
(c) Means of compensation for probe current fluctuations:
- feedback to the gun to control the probe current, or
- feedback to the signal video gain, or
- both, or
- some other means?
(d) If probe current feedback is used, where is it applied, and how are effects on the optics avoided (defocus, deflection, etc.)?
Authors: (a) Flashing cycle is about once per day. (b) Probe current fluctuations are about 8% peak-to-peak during SEM observation. (c) These fluctuations are compensated through a ratio amplifier between the probe current and the secondary electron signals (video signals). (d) Probe current feedback is not used.

J.C. Wiesner: Please provide an idea of available probe currents as a function of final probe size and of accelerating voltage.
Authors: The resolution is not yet estimated directly with respect to the probe current, however, the probe current, I_p, is evaluated as follows:

$$I_p = k \frac{V_0}{V_1} Mg^2 M^2 \alpha_0^2 I_e$$

here, k is a constant depending upon the gun brightness, V_0 is the accelerating voltage, V_1 is the driving voltage for the field emission on the first anode, I_e is an emission current. Mg is magnification at the Butler-lens, M is an integrated magnification of a condenser and objective lenses, α_0 is an incident angle of the focussed probe onto the specimen.

J.C. Wiesner: Please explain a little more quantitatively the calculation of spot size in the low- and high-voltage limits. Describe the agreement between calculation and observation. What is the magnification, overall, from source to specimen? What is the magnification of the final lens alone? What are the contributions of the preceding lenses (condenser and intermediate) to the final probe size? If the overall magnification for high currents is close to unity, how can the source size be neglected?
Authors: Quantitative discussion of spot size has been covered above. In general, the observable resolution at the higher voltage range is less than that of the calculated probe size except for high contrast specimens, for example, fine Pt particles on carbon (see Fig.8a). This discrepancy may be caused mainly by the non-local nature of the secondary information, especially for low contrast materials. On the other hand, we could observe the sample with the estimated resolution at lower accelerating voltage. We need, either way, more discussion based on diverse experiments to clarify the resolution limit of the UHR SEMs.

Electron optical magnification, overall, including Butler-lens is about $1/20 \sim 1/50$ in our case. Since the demagnification to the final objective lens is about 1/30, the disk of confusion caused by the aberration (from sources other than the objective lens) is so small that it could be neglected. Also, the source size of the field emission gun has little effect on the final probe size because the total magnification of the optics is smaller than unity.

J.C. Wiesner : Please describe the performance of the SEM in the presence of, say, 5 milligauss ambient magnetic AC fields. Please describe the vibration isolation and immunity.
Authors: Allowance for the outside disturbance is: 1mG r.m.s. for AC fields and 0.3 μm peak-to-peak at 3Hz or 2 μm p-p at 5Hz with rubber isolation for the vibrations.